

# The influence of relativistic effects on electronic energy levels in metal tetraiodides $MI_4$ ( $M = Ti, Zr, Hf, Th$ )<sup>☆</sup>



Jennifer C. Green<sup>\*</sup>, Russell G. Egdell

Department of Chemistry, University of Oxford, Inorganic Chemistry Laboratory, South Parks Road, Oxford OX1 3QR, UK

## ARTICLE INFO

### Article history:

Received 12 January 2015

Accepted 19 March 2015

Available online 27 March 2015

### Keywords:

Photoelectron spectroscopy

Relativistic effects

Group 4 iodides

Spin-orbit coupling

Density Functional Theory

## ABSTRACT

The influences of scalar relativistic effects and spin orbit coupling on electronic energy levels in  $TiI_4$ ,  $ZrI_4$ ,  $HfI_4$  and  $ThI_4$  have been explored by density functional theory. Calculated ionization energies are compared with previously published He(I) and He(II) photoelectron spectra of  $TiI_4$ ,  $ZrI_4$  and  $HfI_4$  and with new experimental data for  $ThI_4$ .

© 2015 Elsevier Ltd. All rights reserved.

## 1. Introduction

There is a growing realization that relativistic effects have a strong influence on the energetics, bonding and functional properties of compounds of the heavy elements [1,2]. For example it has recently been shown that the unusual quasi-linear stereochemistry found in  $HgO$  arises from relativistic stabilization of the valence 6s orbitals of Hg along with indirect destabilization of the Hg 5d levels [3]. The consequent small separation between the 5d and 6s orbitals then allows oxygen mediated mixing between them in the  $D_{4h}$  coordination environment: shallow core d level mixing with O 2p levels is much less pronounced in  $ZnO$  and  $CdO$  where the d levels are deeper in energy and these oxides have respectively regular tetrahedral and octahedral coordination around the metal [4]. Elsewhere Pykko and coworkers have explored the energetics of the lead acid battery using first principles calculations of thermodynamic parameters and conclude that the battery voltage of around 2 V would be very much lower in the absence of relativistic stabilization of the 6s levels of Pb [5]. More recently relativistic stabilization of Pb 6s orbitals has been shown to be very important in determining the optical properties of lead-based perovskite iodides now exciting great interest as absorber materials in a new generation of solar cells [6–8].

Developments in computational techniques have allowed relativistic calculations to be performed on increasingly more complex

molecules [9–11] and solids [8]. However it is important to benchmark the approaches now being used against experimental data for simple molecular systems. Here we explore the influence of scalar relativistic effects and spin–orbit coupling on the molecular electronic energy levels in the simple tetraiodides  $TiI_4$ ,  $ZrI_4$ ,  $HfI_4$  and  $ThI_4$ . The calculated molecular ionization energies are compared with previously published photoelectron spectra of the three transition metal halides [12]. The paper also presents experimental He(I) and He(II) photoelectron spectra of  $ThI_4$ . The dominant scalar effect transpires to be stabilization of the molecular  $a_1$  level in  $HfI_4$  and  $ThI_4$ , paralleling stabilization of the atomic 6s and 7s orbitals in Hf and Th respectively. Spin–orbit coupling in these molecules involves a complex interplay between spin–orbit coupling based on iodine with an increasingly important contribution from the metal atom as one progresses through the series from  $TiI_4$  to  $ThI_4$ .

## 2. Experimental

$ThI_4$  was prepared by direct combination of the elements. A weighed lump of the metal (ca. 2 g) was placed in a quartz tube (~1.5 cm OD) and a constriction was worked into the upper end of the tube. The tube was dried under dynamic vacuum and a stoichiometric quantity of iodine was then sublimed from another vessel onto the cooled (liquid  $N_2$ ) metal. The tube was then sealed at the constriction. Reaction was initiated by radio-frequency induced heating and was sustained until the thorium had completely reacted with the iodine. Analysis: % I calc. 68.6, found 68.3.

PE spectra were measured on a Perkin-Elmer PS 16/18 spectrometer, modified for He(II) measurements by the inclusion of a

<sup>☆</sup> We dedicate this paper to Professor Mike Mingos, an esteemed colleague and friend.

<sup>\*</sup> Corresponding author. Tel.: +44 01865 272600.

E-mail address: [jennifer.green@chem.ox.ac.uk](mailto:jennifer.green@chem.ox.ac.uk) (J.C. Green).

**Table 1**  
Calculated and experimental interatomic distances (Å) for  $MI_4$ .

M	Method	Ti	Zr	Hf	Th
M–I	Exp	2.546 [21]	2.660 [21]	2.662 [21]	2.91 [22]
	NR	2.58	2.73	2.72	3
	ZORA	2.57	2.71	2.69	2.95
	SO	2.57	2.71	2.69	2.95
I–I	ZORA/SO	4.19	4.43	4.39	4.82

**Table 2**  
Kohn–Sham orbital energies (eV) for  $MI_4$  without and with the inclusion of scalar relativistic effects.

$MI_4$	$TiI_4$		$ZrI_4$		$HfI_4$		$ThI_4$	
	NR	ZORA	NR	ZORA	NR	ZORA	NR	ZORA
$1t_1$	–6.88	–6.79	–7.03	–6.97	–7.05	–6.95	–7.29	–7.14
$3t_2$	–7.73	–7.63	–7.67	–7.61	–7.69	–7.65	–7.23	–7.28
$1e$	–7.94	–7.84	–7.89	–7.92	–8.03	–7.92	–7.67	–7.69
$2t_2$	–8.28	–8.21	–8.38	–8.34	–8.41	–8.34	–7.96	–8.06
$2a_1$	–9.01	–9.01	–8.81	–8.93	–8.89	–9.41	–8.00	–8.57

hollow cathode discharge lamp and high current power supply (Helectros Developments). The discharge lamp heats the sample, which was contained in a quartz tube. An adequate vapour pressure for measurement of spectra was obtained with a sample temperature of 500 °C.

Samples were introduced into the spectrometer under an argon filled dry bag. Spectra were calibrated using  $He(I\alpha)$ ,  $He(I\beta)$  and  $He(II\alpha)$  excited signals of admixed inert gases and  $N_2$ . Band areas were corrected to allow for variation in analyzer transmission function with electron kinetic energy.

### 3. Computational methods

Density functional calculations were carried out using the Amsterdam Density Functional program suite, ADF 2012.01 [13,14]. TZP basis sets were used with triple- $\xi$  accuracy sets of Slater-type orbitals [15,16], with polarization functions added to all atoms. Relativistic corrections were made using the ZORA (zero-order relativistic approximation) formalism, and the spin-orbit formalism. The BP functional was employed [17–20]. The core electrons were frozen up to 2p for Ti, 3d for Zr and 4p for Hf and I and 4f for Th. The geometries of  $MI_4$  ( $M = Ti, Zr, Hf, Th$ ) were optimized with a  $T_d$  symmetry constraint. Frequency calculations confirmed energy minima. The effect of freezing the core orbitals was tested with single point all electron spin-orbit calculations. Only small differences in orbital energies were found (see ESI). Vertical ionisation energies were calculated by direct unrestricted calculations on the molecular ions in their ground and appropriate excited states, and subtraction of the energy of the neutral molecule. Cartesian coordinates for the optimized structures are given in the electronic Supplementary information.

### 4. Results and discussion

Density functional calculations were carried out for the four  $MI_4$  molecules ( $M = Ti, Zr, Hf, Th$ ) at three different levels. The first neglected relativistic effects (NR), the second included scalar relativistic effects (ZORA) and the third included the effect of spin orbit coupling (SO). The geometries of the four  $MI_4$  molecules were optimized at these three levels. The resulting tetrahedral geometries are given in Table 1. Inclusion of relativistic effects reduce the calculated M–I bond length, the effect increasing down the group. Addition of spin-orbit coupling makes little difference to the geometry.

**Table 3**  
Kohn–Sham orbital energies (eV) and Mulliken populations for  $MI_4$ .

		$1t_1$	$3t_2$	$1e$	$2t_2$	$2a_1$
$TiI_4$	Energy	–6.79	–7.63	–7.84	–8.21	–9.01
	%I 5p	100	84	75	71	81
	%Ti 3d		9	25	19	
	%Ti 4s					15
	%Ti 4p		6		6	
$ZrI_4$	Energy	–6.97	–7.61	–7.92	–8.34	–8.93
	%I 5p	100	89	74	73	80
	%Zr 4d		4	27	21	
	%Zr 5s					15
	%Zr 5p		8		1	
$HfI_4$	Energy	–6.95	–7.65	–7.92	–8.34	–9.41
	%I 5p	100	88	75	74	73
	%Hf 5d		5	24	19	
	%Hf 6s					22
	%Hf 6p		7		3	
$ThI_4$	Energy	–7.14	–7.28	–7.69	–8.06	–8.57
	%I 5p	92	94	80	73	76
	%Th 5f	7			2	3
	%Th 6d			20	20	
	%Th 7s					17
	%Th 7p		4			

### 5. Electronic structure

With neglect of spin-orbit coupling, the 32 valence electrons of the Group 4 tetrahalides occupy orbitals with the general ordering  $1t_1 > 3t_2 > 2e > 2t_2 > 2a_1 > 1t_2 > 1a_1$

The  $1a_1$  and  $1t_2$  orbitals are predominantly I 5s in character and are not considered in the subsequent discussion as they are not observed in the experimental spectra.

The effect of inclusion of scalar relativistic effects (ZORA) is shown in Table 2.

The most striking effect on the orbital energies is the stabilization of the  $2a_1$  level for  $HfI_4$  and  $ThI_4$  on inclusion of the scalar corrections. Kohn–Sham orbital energies, calculated with scalar relativistic corrections but without spin-orbit coupling, and their compositions are given in Table 3 and plotted in Fig. 1a.

In all cases the orbital ordering is the same. The spread of energies is strongly influenced by through space interactions between the I 5p orbitals and is therefore a function of the I–I distance. Thus the  $1t_1$  orbital involves out of phase through space antibonding interactions which become less important as the I–I separation increases. It follows that  $TiI_4$  has the highest energy  $1t_1$  orbital. Conversely, the  $2a_1$  orbital involves in-phase through space interactions and this orbital is at lower energy in  $TiI_4$  than in  $ZrI_4$  and  $ThI_4$ . However the  $2a_1$  orbital is much more stable in  $HfI_4$  than in  $ZrI_4$ , even though the bond lengths are almost identical in the two compounds. The increased stability of the  $2a_1$  orbital of  $HfI_4$  mirrors stabilisation of the 6s orbital in Hf as compared to Zr and is influenced by two effects. Hf occurs in the periodic table after the filling of the 4f shell. The 4f orbitals have no radial nodes and are unable to shield the highly penetrating 6s orbitals from the increase in nuclear charge across the lanthanide series. At the same time the 6s orbital in atomic Hf is strongly stabilised by scalar relativistic effects, which become increasingly important with increasing atomic number. Thus the valence s ionisation energies in Ti, Zr and Hf are respectively 6.828 eV, 6.634 eV and 6.825 eV. The  $2a_1$  bonding orbitals have a contribution from their respective metal ns orbitals (Table 3) and thus the increase from  $ZrI_4$  to  $HfI_4$  mirrors the increase in the atomic ionisation energy.

The energies of the orbitals tend to rise for all of the orbitals in  $ThI_4$ , apart from the  $1t_1$  orbital, which is the most stable of the Group IV set. The stability maybe in part a consequence of the

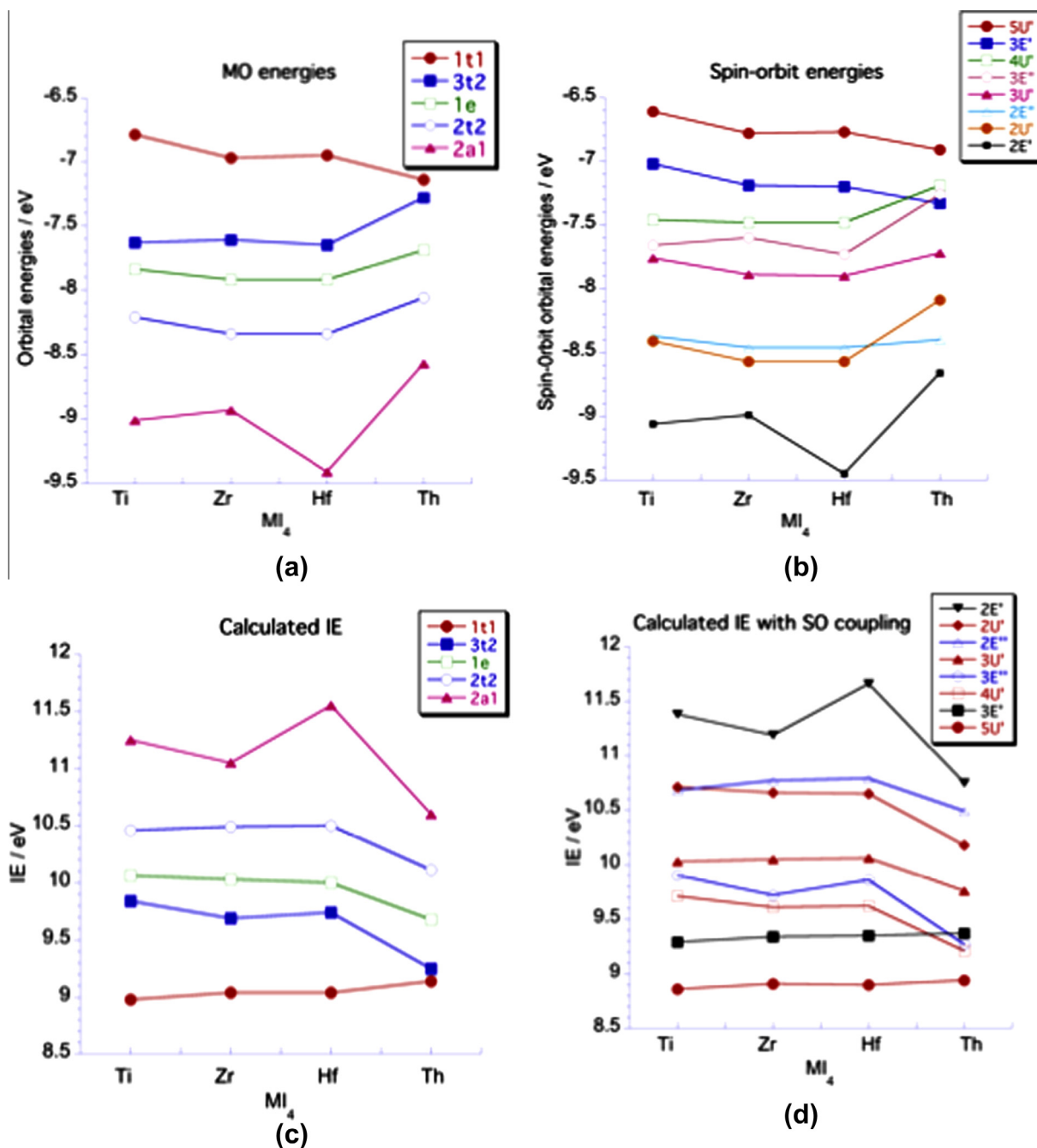


**Fig. 1.** (a) Kohn–Sham orbital energies (ZORA) for  $M_4$  (b) Kohn–Sham orbital energies with spin–orbit corrections (SO) for  $M_4$  (c) calculated IE (ZORA) for  $M_4$  (d) calculated IE including SO coupling (SO) for  $M_4$ . (Colour online.)

greater I–I distance but, whereas the  $1t_1$  combination has no symmetry match among the valence orbitals of the d-block metals, Th is able to form a bonding combination with its 5f orbitals, and the calculations suggest a small (7%) contribution to the MO in this case (Table 3).

Table 3 reveals a high degree of I 5p character to all orbitals consistent with the bond polarity. The  $2a_1$  orbital in  $ThI_4$  has a relativistic stabilisation (0.57 eV) even bigger than that in  $HfI_4$  (0.52 eV). The influence of relativistic effects on the energy of the 7s orbital in Th may be discerned by comparing the atomic ionisation energies of Ce (5.539 eV) and Th (6.307 eV). There is an increase of 0.768 eV despite an increase in the principal quantum number from 6 to 7.

Representative iso-surfaces for the orbitals of  $HfI_4$  are shown in Fig. 2.

In principle there is no  $\sigma\pi$  separability for tetrahedral molecules but iso-surfaces show that the  $3t_2$  orbital is principally  $\pi$  in character and non-bonding, and  $2t_2$  principally  $\sigma$  and bonding. The  $3t_2$  orbitals show a small amount of mixing with the metal ( $n-1$ )d and np orbitals but the principal  $\sigma$  bonding interaction is enshrined in the  $2t_2$  orbital between I 5p and metal ( $n-1$ )d orbitals, the metal np orbitals have a very minor role. The 2e orbital gives  $\pi$  bonding exclusively with the metal ( $n-1$ )d orbitals.

It is now well established that for early actinides the shallow core 6p shell can also be involved in metal–ligand bonding [23,24]. Its energy and radial distribution are favorable for mixing

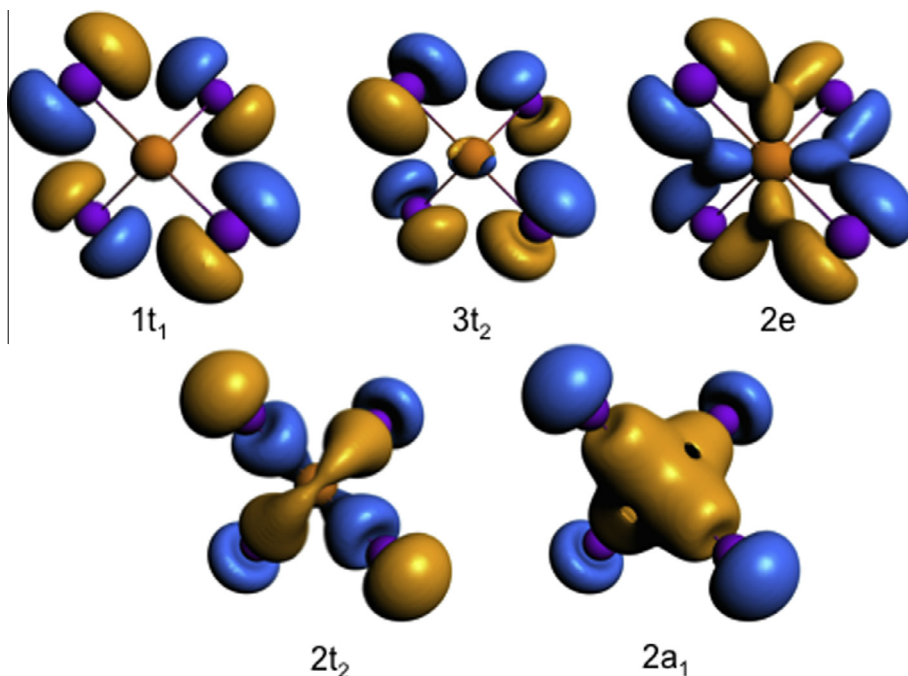


Fig. 2. Isosurfaces for the top occupied Kohn–Sham orbitals of HfI<sub>4</sub> observed along a C<sub>2</sub> axis. (Colour online.)

Table 4

Descent of symmetry from T<sub>d</sub> to T<sub>d</sub><sup>h</sup>.

T <sub>d</sub>	T <sub>d</sub> <sup>h</sup>
A <sub>1</sub>	E' (E <sub>1/2</sub> )
E	U' (U <sub>3/2</sub> )
T <sub>1</sub>	U' + E' (U <sub>3/2</sub> + E <sub>1/2</sub> )
T <sub>2</sub>	U' + E'' (U <sub>3/2</sub> + E <sub>5/2</sub> )

Table 5

Energies (eV) of the spin-orbitals of MI<sub>4</sub>.

M	5U'	3E'	4U'	3E''	3U'	2E''	2U'	2E'
Ti	-6.61	-7.02	-7.46	-7.66	-7.76	-8.37	-8.41	-9.06
Zr	-6.78	-7.19	-7.48	-7.6	-7.89	-8.57	-8.46	-8.99
Hf	-6.77	-7.20	-7.48	-7.73	-7.90	-8.57	-8.46	-9.45
Th	-6.91	-7.33	-7.19	-7.26	-7.72	-8.40	-8.09	-8.66

with the valence orbitals of smaller ligands. In the case of our calculations on ThI<sub>4</sub> the 6p orbitals were included in the basis set but gave no contribution to the t<sub>2</sub> set of orbitals, which instead mixed to some extent with the 7p orbitals. Presumably the greater bond length and the diffuse nature of the I 5p orbitals results in poor overlap with the pseudo core orbitals of the Th 6p set. The behavior found here for ThI<sub>4</sub> contrasts with that found for both HfCl<sub>4</sub> [25] and OsO<sub>4</sub> [26,27], where mixing with shallow core 5p levels gives measurable spin orbit splitting in the outer occupied t<sub>2</sub> level.

## 6. Spin-orbit energy levels

The effects of spin-orbit coupling on metal tetrahalides has been considered previously [12,24,28,29]. Inclusion of the spin orbit effects splits the <sup>2</sup>T levels as shown in the descent of symmetry table (Table 4).

Before looking at the calculation results it is useful to summarize the conclusions from a phenomenological approach developed

Table 6

Calculated splittings of the orbital energy levels (eV) and in parenthesis shifts in the mean of SO split energy levels (eV) on inclusion of spin-orbit coupling for MI<sub>4</sub>.

M	1t <sub>1</sub>	3t <sub>2</sub>	1e	2t <sub>2</sub>	2a <sub>1</sub>
Ti	0.41 (-0.07)	0.20 (-0.1)	0 (-0.08)	-0.04 (0.19)	0 (0.05)
Zr	0.41 (-0.05)	0.12 (-0.09)	0 (-0.03)	0.11 (0.19)	0 (0.06)
Hf	0.43 (-0.04)	0.25 (-0.09)	0 (-0.02)	0.11 (0.16)	0 (0.03)
Th	0.42 (-0.09)	0.05 (-0.07)	0 (0.03)	0.31 (0.13)	0 (0.09)

-means less stable, + means more stable.

Table 7

Calculated ionization energies (eV) for MI<sub>4</sub> molecules.

M	1t <sub>1</sub>	3t <sub>2</sub>	1e	2 t <sub>2</sub>	2a <sub>1</sub>
Ti ZORA	8.98	9.84	10.06	10.46	11.25
Ti SO	8.86 U'	9.71 U'	10.03 U'	10.68 E''	11.38 E'
	9.84 E'	9.90 E''		10.71 U'	
Zr ZORA	9.04	9.69	10.03	10.49	11.05
Zr SO	8.91 U'	9.61 U'	10.05 U'	10.66 U'	11.19 E'
	9.34 E'	9.72 E''		10.77 E''	
Hf ZORA	9.04	9.74	10.00	10.50	11.55
Hf SO	8.9 U'	9.62 U'	10.06 U'	10.65 U'	11.66 E'
	9.35 E'	9.86 E''		10.79 E''	
Th ZORA	9.14	9.25	9.68	10.11	10.6
Th SO	8.94 U'	9.21 U'	9.76 U'	10.18 U'	10.75 E'
	9.37 E'	9.27 E''		10.49 E''	

many years ago [28]. In the absence of interaction between the I 5p orbitals and orbitals of the central atom (as is the case for the transition metal iodides) and further ignoring the need for normalization due to I-I overlap, the 1t<sub>1</sub> level should be split by  $-3\zeta_{I5p}/4$ , where  $\zeta_{I5p}$  is the spin-orbit coupling constant for I 5p orbitals. This value is basically half that found for a free iodine atom and predicts the U' ionic state to lie at lower energy than the E' state. This simple expression is potentially modified in the case of Th as the t<sub>1</sub> orbitals are no longer exclusively I 5p based, but the Th 5f orbital spin-orbit splitting and the contribution to the 1t<sub>1</sub> orbital

are too small to have a noticeable effect. The value of  $\zeta_{16p}$  for an I atom is 0.628 eV [30] giving an estimate of 0.47 eV for the  $5U' - 3E'$  separation.

The splitting of the  $t_2$  orbitals is considerably more complex as the magnitude and sign of the splitting are a function of the degree of  $\sigma\pi$  mixing and also the contribution from metal d and p orbitals may well be significant. However for a pure I 6p system with no I-metal overlap and neglecting the normalization constant arising from I–I overlap, a pure  $t_2(\pi)$  set would be split by  $-3\zeta_{16p}/4$  and a  $t_2(\sigma)$  set would have a zero splitting. Mixing between the two can however lead to a full restoration of the atomic spin orbit splitting found in a free I atom (i.e.  $-3\zeta_{16p}/2$ ) in the uppermost  $t_2$  level where  $\sigma$  and  $\pi$  contributions are out-of-phase and a splitting of half this magnitude with the opposite phase (i.e.  $+3\zeta_{16p}/4$ ) in the lower in-phase  $t_2$  combination, where the  $U'$  ionic state is now at higher energy than the  $E''$  state. This situation pertains when the wavefunctions for the two  $t_2$  combinations can be written as:

$$3t_2 = \sqrt{\frac{2}{3}}t_2(\pi) - \sqrt{\frac{1}{3}}t_2(\sigma)$$

$$2t_2 = \sqrt{\frac{1}{3}}t_2(\pi) + \sqrt{\frac{2}{3}}t_2(\sigma)$$

The results for the orbital energies with spin–orbit coupling (SO) included are given in Table 5. The energy levels are plotted in Fig. 1b. Table 6 gives the calculated splittings of the various levels and the degree to which the energy mean of the split SO levels shifts from the ZORA value.

Due to I 5p dominance of orbital composition the I 6p orbitals are expected to dominate the SO splitting. The  $1t_1$  splitting is consistent down the group with  $5U' < 2E'$  and the energy trend of the spin–orbit components reflects that of the parent orbital. The magnitude of the splitting is 0.41–0.43 eV which compares favorably with the 0.47 eV estimated above. The  $1e$  and  $2a_1$  levels are unsplit and relatively unshifted.

With the  $3t_2$  and  $2t_2$  levels, possible interaction between the sets should be considered. If splitting for  $3t_2(\pi)$  is  $U' < E''$  and for  $2t_2(\sigma)$   $E'' < U'$ , interaction between  $E''$  levels will reduce the SO splitting of both sets, leading to low values calculated for  $t_2$  splittings. There is evidence for this in that the means for the spin–orbit components of these two sets show greater shifts than the other means and move apart. The significantly larger splitting of the  $2t_2$  orbital for  $\text{ThI}_4$  is attributed to the admixture of the Th 6d orbitals, the spin–orbit coupling constant for Th 6d being sufficiently large for only a 20% contribution to be effective. The spin–orbit coupling constant for  $\text{Pa}^{4+}$  has been measured as 0.23 eV [31], and has been calculated as 0.38 eV [32], that for  $\text{Th}^{4+}$  will be less as the nuclear charge is less.

## 7. Ionization energy calculations

IE calculations were performed both with and without spin–orbit coupling (ZORA and SO). The calculated ionization energies are given in Table 7 and plotted in Fig. 1(c) and (d).

From inspection of Fig. 1 it is evident that the trends in calculated IE are the inverse of the trends in orbital energies and hence they have the same underlying causes.

## 8. Assignment of photoelectron spectra

Photoelectron spectra of the transition metal tetraiodides  $\text{MI}_4$  ( $M = \text{Ti}, \text{Zr}, \text{Hf}$ ) have been reported previously [12]. That of  $\text{ThI}_4$  has not been published previously, although experimental data for the other thorium tetrahalides is available [24,29]. The He I and He II spectra of  $\text{TiI}_4$  are shown in Fig. 3. A listing of identifiable vertical ionization energies for all four iodides is given in Table 8 together with possible band assignments.

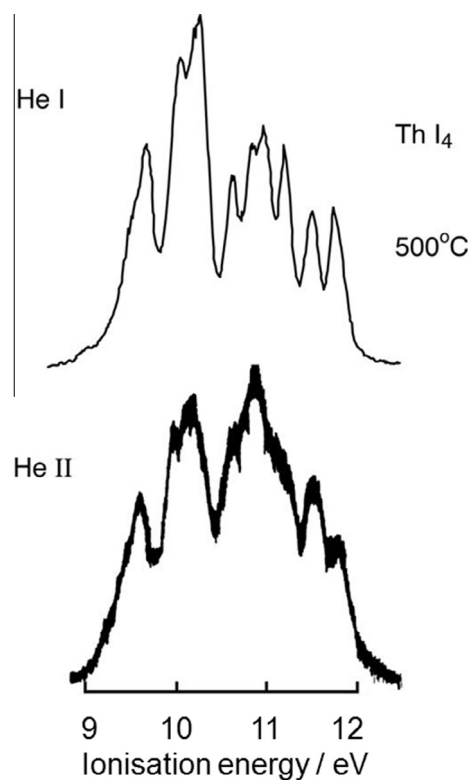


Fig. 3. He I ( $h\nu = 21.2$  eV) and He II ( $h\nu = 40.8$  eV) photoelectron spectra of  $\text{ThI}_4$ .

Table 8

Experimental vertical ionization energies (eV) for  $\text{MI}_4$  molecules and suggested assignments.

	Ti	Zr	Hf	Th
a	9.22(sh), 9.32 5U'	9.49(sh), 9.61 5U'	9.48(sh), 9.57 5U'	a 9.47(sh), 9.67 5U'
b	9.77 3E'	10.03 3E'	10.05 3E'	b 10.02 4U'
c	10.32 4U' 10.45 3E''	10.33, 10.51 4U' 10.51 3E''	10.37, 10.56 4U' 10.67 3E''	c 10.26 3E'' + 3E' 10.62, 10.82 3U'
d	10.68 3U' 11.19 2E''	10.77, 10.96 3U' 11.35, 11.49 2U'	10.82, 10.95 3U' 11.45, 11.56 2U'	d 10.97, 11.19 2U' 11.49 2E''
e	11.34 2U' 11.92 2E'	11.68 2E'' 12.00 2E'	11.68 2E'' 12.47 2E'	e 11.76 2E'

Table 9

Relative band intensities in the He I and He II spectra of  $\text{MI}_4$ .

	$\text{TiI}_4$		$\text{ZrI}_4$		$\text{HfI}_4$		$\text{ThI}_4$	
	He I	He II						
a	2.0 (2)	2.0	2.0 (2)	2.0	2.0 (2)	2.0	2.0 (2)	2.0
b	1.1 (1)	1.3	1.0 (1)	1.0	1.0 (1)	1.1	4.4(4)	4.5
c	5.2 (5)	9.2	4.6 (5)	17.1	5.1 (5)	9.1	4.2(4)	6.4
d	3.4 (3)	5.8	2.8 (3)	12.8	3.7 (3)	6.3	0.8 (1)	1.8
e	0.9 (1)	1.7	1.1 (1)	2.7	0.8 (1)	1.6	0.9 (1)	0.8

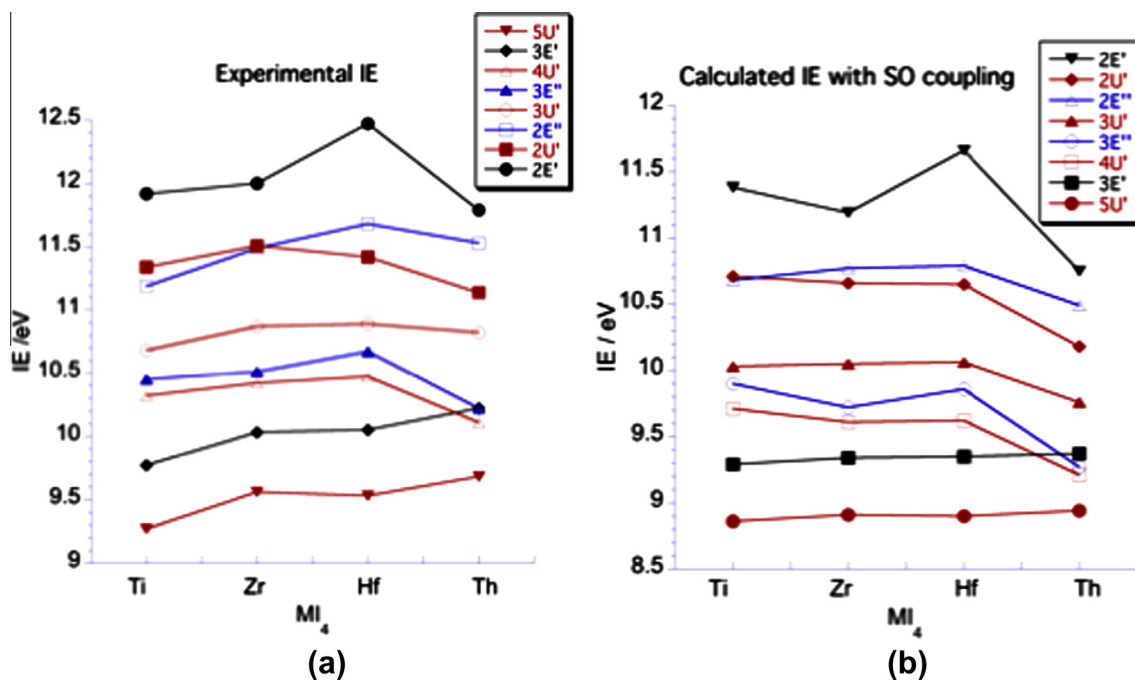


Fig. 4. Comparison of experimental (a) and calculated (b) vertical ionization energies (eV) of MI<sub>4</sub> M = Ti, Zr, Hf and Th. (Colour Online.)

The eight spin orbits, which ionize in the energy region below 13 eV, should give rise to eight primary ionization processes. However in some of the spectra more than eight features are identifiable. This is a consequence of Jahn–Teller (J–T) splitting of the <sup>2</sup>U' states in the molecular ion. We may anticipate that such J–T splitting is greater for states involving a hole with bonding character than for non-bonding ones such as <sup>2</sup>T<sub>1</sub> states.

Changes in relative intensity of bands with photon energy can identify the states arising from ionization of electrons from orbitals with metal d character as these tend to increase in relative intensity in the He II spectra. The dominance of I character in the orbitals leads to band intensities in the He I spectra reflecting the degeneracies of the contributing states. Both these criteria are used to assist band assignment. Band intensities are given in Table 9.

The number of states that must be assigned to each region is given in parentheses in Table 9. We may also conclude that regions c and d arise from orbitals with metal d character.

Assignment of the 5U' and 2E' states as to the lowest and highest IE bands respectively is unambiguous, as is the 3E' state to the second band b for M = Ti, Zr and Hf. For ThI<sub>4</sub>, the assumption of a SO splitting similar to its congeners places the 3E' states within the band at 10.22 eV.

The He I/He II intensity variations suggest that the 2E'', 3U' and 4U' states contribute to the higher IE bands in regions d and c, though for the d block elements the lower IE region of band c shows a smaller intensity increase with photon energy. The intensity considerations together with the calculations suggest the assignments given in Table 8.

### 9. Comparison of experimental and calculated ionization energies

The experimental and calculated ionization energies are shown in Fig. 4. Where splitting of a <sup>2</sup>U' state is observed the mean is plotted in Fig. 4. Overall the calculated IE are too low when compared with experiment [33]. Such underestimates are common when using density functional techniques and the  $\Delta$ SCF method, the discrepancy normally increasing with increasing IE. In general the

calculations reproduce well the trends observed in the spectra. In particular the predicted groupings of the bands in the calculations concur with the intensity observations, notably the 2:1:5:3:1 pattern observed for the d-block elements as opposed to the 2:4:4:1:1 pattern for ThI<sub>4</sub> (Table 9). In addition the observed increases in relative intensity of bands in the He II spectra are in the calculations associated with spin-orbitals derived from orbitals with the highest d content, 1e and 2t<sub>2</sub>. The trends down the group of the bands 5U', 3E' and 2E' which may be identified without ambiguity are very well reproduced by the calculations.

### 10. Concluding remarks

The excellent agreement between the observed pattern of experimental ionization energies for the metal tetraiodides shown in Fig. 4 and those calculated by density functional theory methods after inclusion of both scalar relativistic effects and spin-orbit coupling give one considerable confidence in the ability of current computational techniques to explore and understand the complexities of electronic structure in complex heavy atom systems. Publication of experimental photoelectron spectra of ThI<sub>4</sub> completes the experimental data set of photoelectron spectra for the thorium tetrahalides.

Molecular photoelectron spectroscopy should continue to provide an important technique for benchmarking electronic structure calculations as is the case for solid state materials.

### Acknowledgements

We thank the SRC for the purchase of a spectrometer and the Salter's Company for a scholarship (R.G.E.). We also gratefully acknowledge the contribution of Tony Orchard to the inception of this work.

### Appendix A. Supplementary data

Supplementary data associated with this article can be found, in the online version, at <http://dx.doi.org/10.1016/j.poly.2015.03.014>.

## References

- [1] P. Pyykko, *Ann. Rev. Phys. Chem.* 63 (2012) 45.
- [2] M. Barysz, Y. Ishikawa (Eds.), *Relativistic Methods for Chemists*, Springer, Dordrecht, 2010.
- [3] P.A. Glans, T. Learnmonth, K.E. Smith, J. Guo, A. Walsh, G.W. Watson, F. Terzi, R.G. Egdell, *Phys. Rev. B* 71 (2005) 235109.
- [4] P.A. Glans, T. Learnmonth, C. McGuinness, K.E. Smith, J.H. Guo, A. Walsh, G.W. Watson, R.G. Egdell, *Chem. Phys. Lett.* 399 (2004) 98.
- [5] R. Ahuja, A. Blomqvist, P. Larsson, P. Pyykko, P. Zaleski-Ejgierd, *Phys. Rev. Lett.* 106 (2011) 018301.
- [6] X. Zhu, H.B. Su, R.A. Marcus, M.E. Michel-Beyerle, *J. Phys. Chem. Lett.* 5 (2014) 3061.
- [7] E. Menendez-Proupin, P. Palacios, P. Wahnon, J.C. Conesa, *Phys. Rev. B* 90 (2014) 045207.
- [8] F. Brivio, K.T. Butler, A. Walsh, M. van Schilfgaarde, *Phys. Rev. B* 89 (2014) 155204.
- [9] N. Kaltsoyannis, B.E. Bursten, *J. Organomet. Chem.* 528 (1997) 19.
- [10] L. Andrews, X. Wang, Y. Gong, G.P. Kushto, B. Vlasisavljevich, L. Gagliardi, *J. Phys. Chem. A* 118 (2014) 5289.
- [11] S.G. Minasian, J.M. Keith, E.R. Batista, K.S. Boland, D.L. Clark, S.A. Kozimor, R.L. Martin, D.K. Shuh, T. Tylliszczak, *Chem. Sci.* 5 (2014) 351.
- [12] R.G. Egdell, A.F.J. Orchard, *Chem. Soc. Farad. II* 73 (1977) 485.
- [13] SCM, 2002.2 ed., *Theoretical Chemistry*, Vrije Universiteit: Amsterdam, 2002.
- [14] G. te Velde, E.J. Baerends, *J. Comp. Phys.* 99 (1992) 84.
- [15] J.C. Slater, *Theory of Molecules and Solids. Vol. 4: The self-Consistent Field for Molecules and Solids*, Mc-Graw-Hill, New York, 1974.
- [16] J.S. Slater, *The Calculation of Molecular Orbitals*, Wiley, New York, 1979.
- [17] A.D. Becke, *Phys. Rev. A* 38 (1988) 2398.
- [18] J.P. Perdew, *Phys. Rev. B* 33 (1986) 8822.
- [19] J.P. Perdew, *Phys. Rev. B* 34 (1986) 7046.
- [20] S.H. Vosko, L. Wilk, M. Nusair, *Can. J. Phys.* 58 (1980) 1200.
- [21] G.V. Girichev, E.Z. Zazorin, N.I. Giricheva, K.C. Krasnov, V.Zh. Spiridovnov, *Strukt. Khim.* 18 (1977) 42.
- [22] R.J.M. Konings, D.L. Hildebrand, *J. Alloys Comp.* 271 (1998) 583.
- [23] R.G. Denning, J.C. Green, T.E. Hutchings, C. Dallera, A. Tagliaferri, K. Giarda, N.B. Brookes, L. Braicovich, *J. Chem. Phys.* 117 (2002) 8008.
- [24] J.M. Dyke, N.K. Fayad, A. Morris, I.R. Trickle, *J. Chem. Phys.* 72 (1980) 3822.
- [25] N. Kaltsoyannis, *Chem. Phys. Lett.* 274 (1997) 405.
- [26] B.E. Bursten, J.C. Green, N. Kaltsoyannis, *Inorg. Chem.* 33 (1994) 2315.
- [27] P. Pyykkö, J. Li, T. Bastug, B. Fricke, D. Kolb, *Inorg. Chem.* 32 (1993) 1525.
- [28] J.C. Green, M.L.H. Green, P.J. Joachim, A.F. Orchard, D.W. Turner, *Philos. Trans. R. Soc. A* 268 (1970) 111.
- [29] L.J. Beeching, J.M. Dyke, A. Morris, J.S. Ogden, *J. Chem. Phys.* 114 (2001) 9832.
- [30] M. Montalati, A. Credi, L. Prodi, T. Gandolfi, *Handbook of Photochemistry*, Taylor and Francis, CRC Press, 2006.
- [31] N. Edelstein, W.K. Kot, J.C. Krupa, *J. Chem. Phys.* 96 (1992) 1.
- [32] L. Seijo, Z. Barandiaran, B. Ordejon, *Mol. Phys.* 101 (2003) 73.
- [33] J.C. Green, P. Decleva, *Coord. Chem. Rev.* 249 (2005) 209.